Skin Disease Detection Employing Transfer Learning Approach- A fine-tune VGG-19

BY

Md: Al-Habib Islam
ID: 191-15-2629

AND

S.M Shahriyar
ID: 191-15-2667

This Report Presented in Partial Fulfillment of the Requirements for the Degree of Bachelor of Science in Computer Science and Engineering

Supervised By

Mohammad Jahangir Alam
Senior Lecturer
Department of CSE
Daffodil International University

Co-Supervised By

Al Amin Biswas
Senior Lecturer
Department of CSE
Daffodil International University

DAFFODIL INTERNATIONAL UNIVERSITY

DHAKA, BANGLADESH

FEBRUARY 2023

APPROVAL

This Project/internship titled "**Skin Disease Detection Employing Transfer Learning Approach- A fine-tune VGG-19**", submitted by Md. Al-Habib Islam, ID No: 191-15-2629 and S.M Shahriyar, Id No: 191-15-2667 to the Department of Computer Science and Engineering, Daffodil International University has been accepted as satisfactory for the partial fulfillment of the requirements for the degree of B.Sc. in Computer Science and Engineering and approved as to its style and contents. The presentation has been held on *04/02/2023*.

BOARD OF EXAMINERS

Chairman

Dr. Touhid Bhuiyan
Professor and Head
Department of Computer Science and Engineering
Faculty of Science & Information Technology
Daffodil International University

Internal Examiner

Subhenur Latif
Assistant Professor
Department of Computer Science and Engineering
Faculty of Science & Information Technology
Daffodil International University

Internal Examiner

04.02.23

Md. Sabab Zulfiker
Senior Lecturer
Department of Computer Science and Engineering
Faculty of Science & Information Technology
Daffodil International University

External Examiner

Dr. Md. Sazzadur Rahman
Associate Professor
Institute of Information Technology
Jahangirnagar University

DECLARATION

We hereby declare that, this project has been done by us under the supervision of **Mohammad Jahangir Alam, Senior Lecturer, Department of CSE** Daffodil International University. We also declare that neither this project nor any part of this project has been submitted elsewhere for award of any degree or diploma.

Supervised by:

Jahangir 01.02.23

Mohammad Jahangir Alam
Senior Lecturer
Department of CSE
Daffodil International University

Co-Supervised by:

Al Amin Biswas
Senior Lecturer
Department of CSE
Daffodil International University

Submitted by:

Habib

Md.Al-Habib Islam
ID: 191-15-2629
Department of CSE
Daffodil International University

Shahriyar

S.M Shahriyar
ID: 191-15-2667
Department of CSE
Daffodil International University

ACKNOWLEDGEMENT

First we express our heartiest thanks and gratefulness to almighty God for His divine blessing makes us possible to complete the final year project/internship successfully.

We really grateful and wish our profound our indebtedness to **Mohammad Jahangir Alam,** Senior Lecturer, Department of CSE Daffodil International University, Dhaka. Deep Knowledge & keen interest of our supervisor in the field of "*Deep Learning*" to carry out this project. His endless patience, scholarly guidance, continual encouragement, constant and energetic supervision, constructive criticism, valuable advice, reading many inferior draft and correcting them at all stage have made it possible to complete this project.

We would like to express our heartiest gratitude to **Professor Dr. Touhid Bhuiyan,** Professor and Head, Department of CSE, for his kind help to finish our project and also to other faculty member and the staff of CSE department of Daffodil International University.

We would like to thank our entire course mate in Daffodil International University, who took part in this discuss while completing the course work.

Finally, we must acknowledge with due respect the constant support and patients of our parents.

ABSTRACT

Your skin may become damaged by skin diseases and conditions. These illnesses can cause skin changes such as rashes, inflammation, itching, and other skin changes. While some skin conditions may run in families, others may result from a person's way of life. Pills, creams, ointments, and changes in lifestyle are all potential treatments for skin conditions A large amount of data for model training and improvements in model designs that provide stronger simplifications have led to a rapid advancement of deep learning algorithms for applications involving computer vision. Undesired skin disease regions are eliminated, quality is raised, and the disease is tinted by discarding artifacts, decrease noise, and improving the image. Three augmentation techniques have led to an increase in the number of skin disease images. Several CNN architectures, including VGG16, VGG19, MobileNet, MobileNetV2, and InceptionV3, looked at the augmentation dataset. VGG-19 offers the highest level of accuracy in this case. Following the segmentation of the dermoscopic images, the affected skin cells' features are extracted using a feature extraction technique. Using a convolutional neural network classifier, which is based on deep learning, the extracted features are stratified. The best outcomes were obtained using the hyper-tuned VGG19, which had test and validation accuracy of 99.21% and 99.25%, including both.

TABLE OF CONTENTS

LIST OF FIGURES

LIST OF TABLES

Chapter 1

Introduction

1.1 Introduction

One form of cancer that begins in skin cells and can infiltrate or spread to other bodily areas is skin cancer. The proliferation of aberrant cells is the primary cause of skin cancer. In 2020, it was ranked as the fourth most prevalent cancer [1]. For a variety of reasons, determining the prevalence of skin cancer is a difficult task. Skin cancer comes in a variety of forms, and cancer registries frequently ignore non-melanoma skin cancer [2]. Because surgery or ablation is the most common treatment for skin cancer, registrations are often lacking. The worldwide incidence of skin cancer is probably underestimated due to these variables. The Scandinavian nations in Europe are next in order of reported skin cancer rates, with Australia and New Zealand having the highest rates (33.6 per 100,000 and 33.3 per 100,000, respectively) [3]. The obvious cause of this high prevalence is sun exposure, which is what causes the majority of skin cancers. The human head and neck are the areas where skin malignancies are most often discovered [4]. According to the Global Cancer Observatory, this kind of cancer is less prevalent in Southeast Asia [5, 6]. Skin cancer may be inspected by a dermatologist fairly early on since it manifests on the exterior of the body and is a visible sort of sickness. Early detection of skin cancer lesions lowers morbidity, decreases the cost of healthcare and increases patient survival rates [7]. An unobtrusive examination method called dermo copy allows for a visual assessment of the ρ ISSN: 2502-4752 Indonesian J Elec Eng & Comp Sci, Vol. 99, No. 1, Month 2099: 1-1x 2 surface structure of the skin. The accuracy of the diagnosis relies on the dermatologist's expertise, although this dermo copy-based detection is undoubtedly greater than individual observation-based detection. It is challenging to correctly identify malignant tumors at an early stage due to the dearth of qualified dermatologists [8]. By adding specialists in more effective and efficient treatment, this research helps to identify and classify skin conditions related to Actinic Keratosis, Basal Cell Carcinoma, Dermatofibroma, Melanoma, Nevus, Pigmented Benign Keratosis, Seborrheic Keratosis, Squamous Cell Carcinoma, and

Vascular lesions early on, lowering the risk of death. For a CNN model to implement perfectly, noise and artifact removal is essential and were performed on the dataset. Additionally, the similarity between disease regions and impenetrable skin tissue may make interpretation difficult. Raw image brightness and contrast levels were balanced to make disease lesions more visible. This study proposes the fine-tuned and hyper-tuned VGG19 built on transfer learning and ablation study as a fully automated and efficient deep learning model for the categorization of photos of skin conditions.

1.2 Motivation

This research will enable us to determine whether a person will develop skin cancer early on or not. Skin cancer diseases require early prediction because, if identified at an early stage, they are very easy to treat. All skin tones, including those with darker complexions, are susceptible to developing skin cancer. When skin cells are damaged or get old and die, new skin cells are created. Fortunately, most cases of skin cancer are curable if discovered and treated quickly. Skin cancer affects 20% of Americans at some point in their lives. Every day, 9,500 Americans receive a skin cancer diagnosis. People with skin of color frequently experience skin cancer diagnosis at an advanced stage when it is more challenging to treat.

1.3 Rationale of the Study

To generate deep learning models for detecting skin cancer and classifying images of dermal cells. Deep learning is a method that can be used and learned from. Our primary goals as computer science students were to improve image quality, detection performance, and artifact removal. Through the process, we gained knowledge of various image types. When we used transfer learning on the dataset, we introduced various image processing models.

1.4 Research Questions

We had a lot of questions when we began this research project. There weren't many challenges, but there were some unanswered questions. Like as:

- How will we determine which algorithm is best?
- Which preprocessing technique will we utilize for the image?
- Which part will we employ in order to implement the deep learning algorithm?

1.5 Expected Outcome

- To Detect Skin cancer more efficiently.
- Select algorithm for this dataset.
- Image dataset Preprocess to get the best output from the images.
- Ablation study on the best performance model.
- Configuration of our best performed model.
- Performance analysis and statistical analysis based on the confusion matrix.

1.6 Project Management and Finance

The objective of the project should be clearly stated, along with the specific skin conditions that must be identified and the intended audience for the model. Put together a team with the right expertise to finish the project, including project managers, computer scientists, and medical professionals. Make a thorough plan outlining the procedures to be followed, the deadlines, and the materials needed to finish the project. Calculate all project expenses, including those for personnel, hardware, and software. Determine the project's potential return on investment, and use this data to support the funding and resources given to it.

1.7 Report Layout

A succinct description of the project's aim, strategy, and main conclusions. Describe the history of the detection of skin diseases and the application of transfer learning in this situation. The dataset, pre-trained model (VGG-19), and fine-tuning procedure should all be mentioned in detail as well as the specific strategy used in this project. present and evaluate the model's performance in spotting the intended skin conditions. Add metrics like recall, precision, and accuracy. Interpret the findings and talk about any shortcomings or potential areas for future development.

Chapter 2

Background

2.1 Preliminaries

Give a general overview of the skin diseases this project is focusing on, outlining their causes, symptoms, and standard diagnostic techniques. Describe the idea of transfer learning and any advantages it might have for image classification tasks. Describe the architecture of the VGG-19 model and how well it performs on image classification tasks. Describe how to modify a model that has already been trained for a new task, taking into account the effects of changing the learning rate and the quantity of training samples.

2.2 Related Works

Recently, deep neural networks (DNNs) have demonstrated promise for detecting skin cancer. We provide a method to balance data based on the mutation operator of the Differential Evolution (DE) algorithm since skin cancer datasets are not balanced. In doing so, the method not only provides doctors with a flexible tool to assist them during the skin cancer screening phase, but also achieves promising results with a balanced accuracy of 85% and a recall of 96%. On the Grand Challenge PHDB Melanoma dataset, their model outperformed the baseline model in terms of accuracy and computational effectiveness [9]. Dai et al. [10] also used a CNN to present a skin cancer iOS mobile application. The model was trained using the HAM10000 dataset [11]. The PAD-UFES-20 dataset now includes more skin lesions [12]. An automated technique for melanoma skin cancer detection was proposed by Yu et al. [10] with the use of deep convolutional neural networks (CNNs) and the ISBI 2016 Skin Lesion Analysis toward Melanoma Detection Challenge. Since their network comprised more than 50 levels, they argued that their suggested approach was more accurate than existing topologies. They were able to help their network grow more sophisticated and discriminative traits, which ultimately improved performance. They used extremely deep residual networks for classification and fully convolutional residual networks (FCRN) for segmenting skin lesions in their two-stage framework. 85.5% was the highest reported classification accuracy for this challenge. Yu et al. [11] CNN with

more than 50 layers was built in 2016 for the classification of malignant melanoma cancer using the ISBI 2016 challenge dataset. Using a deep convolutional neural network, Haenssle et al. [12] categorized dermatoscopy melanocytic pictures into a binary diagnostic category in 2018 and reported 86.6% sensitivity and specificity for classification. The best recognition accuracy instance reported varies from 96.0% to 1%. Their approach was distinctive in that it produced a classification accuracy of 85.5% while using far less training data than other authors and a deeper network. Their research provided some evidence that segmentation in a two-stage framework might result in better results than straightforward thermoscopic image alteration. Deep convolutional neural networks were used by Andre Estevan et al. [13] to categorize skin lesions. Pixels and disease labels were the only inputs used to train the CNN on a collection of 129,450 clinical images. Then, using clinical photos that had been verified by a biopsy, they put it to the test against 21 board-certified dermatologists. It has been shown that artificial intelligence systems may be able to identify skin cancer with expertise on par with that of dermatologists. The accuracy for carcinoma pictures was 96%, melanoma images were 94%, and thermoscopic images of melanoma were 91%. The CNN's sensitivity vs. specificity curve was promising, but the rates of false positives and false negatives remained too high to be disregarded. Using deep learning, Jinnai et al. [14] created a method for classifying pigmented skin lesions as skin cancer. The suggested remedy is based on the transfer learning paradigm and the VGGNet convolutional neural network architecture. The experimental results are encouraging: the suggested method achieves a sensitivity value of 78.66% on the ISIC Archive dataset, significantly outperforming the state of the art at the time. According to reports, the clinical diagnosis accuracy for melanoma detection ranges from 65 to 80% [15]. When dermoscopic images are used, the accuracy of diagnosing skin lesions is increased by 49% [16]. This study effectively compares a novel deep learning algorithm for classifying skin lesions against a collection of dermoscopic skin lesion images (the ISIC Archive dataset [17]). It obtained an accuracy value of 81.33% [18] when utilizing the dataset partitioned exactly as the ISBI 2016 Challenge, which would position the suggested technique in the top three in that task. Most importantly, when sensitivity is taken into account, we come up with a score of 78.66%, which is significantly higher than the leader's reported score of 50.7%. Additionally, our precision rating of 79.74% exceeds the best

outcome currently available, which is 63.7%. In order to diagnose skin cancer in 2020, Rehana Ashraf et al. [19] presented a transfer learning-assisted framework based on an intelligent area of interest (ROI) technique. A ROI-based technique aids in the discovery of discriminative features because the photographs used to train the system only include that area. They employed an upgraded version of the k-means method to extract ROIs from the photos. They then used a transfer learning model based on convolutional neural networks (CNN) with data augmentation for ROI photos. While only 23% of the data were used for testing, the remaining 77% were trained on. The ROI-based strategy surpassed earlier methods employing full photos (global features) for classification, with accuracy rates of 97.9% for their first dataset and 97.4% for their second dataset. In order to supplement data in 2018, Goyal et al. [20] proposed region of interest (ROI) detection necroscopic images. They recommended employing two object localization meta-architectures and CNN (Faster-RCNN) to locate ROI skin lesions in thermoscopic pictures. Their skin localization techniques performed better than other skin lesion segmentation techniques, it was found. When used to the ISBI-2017 testing dataset for ROI localization in thermoscopic pictures, FRCNN (Faster-RCNN) Inception V2 outperformed other models with accuracy and recall of 94.5% and 94.3%, respectively. In terms of accuracy and recall, FRCNN also outperformed other datasets that had never been used before, proving its validity. In order to aid in the early identification of melanomas, Ali et al. [21] presented a unique fuzzy method-based multilayer perceptron (F-MLP) system in 2020 for the detection of irregularity in the skin lesion's perimeter. One of the primary indicators of skin cancer is uneven boundaries. Although it has been demonstrated that multilayer perceptrons (MLPs) or artificial neural networks (ANNs) successfully complete supervised learning tasks, their performance may sometimes suffer as a result of how the weights are modified as learning progresses. The vast majority of contemporary classification methods, particularly its typical neural network equivalent, outperformed its proposed method. They found that an 80:20 training-to-testing data ratio, with an accuracy of 95.2%, was the best F-MLP outcome. The suggested fuzzy neural network's disadvantage was that it took a lot longer to train than expected. In mid-2019, Fujisawa et al. [22] presented an autonomous deep learning-based categorization of skin cancer. They made use of the ILSVR2012 dataset, which has 1.2 million photos divided into 1,000 classes. Additionally, they

demonstrated how feature extraction may improve the model's usability and effectiveness. A deep learning-based convolutional neural network (CNN), which can automatically learn from the training picture collection which features are crucial for classification, was the classification method that provided them the best results utilizing the selected feature values. The CNN model outperformed board-certified dermatologists in terms of accuracy for 14-class classification (75%), and for two-class classification (92%). By merging convolutional neural networks and textural characteristics, Seyyed Mohammad Alizadeh et al. [23] created an automated skin cancer diagnosis method using thermoscopic pictures. They utilized the datasets PH2, ISIC 2016, and ISIC 2019. The dimension of texture features was lowered using kernel principal component analysis after they were extracted in order to improve classification performance in the feature extraction-based phase. The images were then classified in the CNN phase using their suggested network and theVGG-19-two CNN models. The outcomes of these two approaches were compared to produce the final result after being put into their ensemble methodology. For three datasets, this automated approach achieved accuracy of 85.2%, 96.7%, and 97.5%, respectively.

2.3 Comparative Analysis and Summary

TABLE 2.2: COMPARATIVE ANALYSIS

Author	Dataset	Algorithm	Accuracy
Our Model	Skin Cancer ISIC	VGG19	98.55%
Haenssle et al. [13]	ISIC(2016)	Inception V3	69.3%
Esteva et al. [20]		GoogLeNet Inception V3 CNN	72.1%
Dorj et al. in Ref. [23].		ECOC SVM	95.1%
Yu et al. [21]	ISBI 2016	CNN	85.5%

2.4 Scope of the Problem

Describe the difficulties that come with spotting skin conditions, particularly with regard to precise diagnosis and prompt treatment. Stress the effect of skin conditions on patients' quality of life and the cost to the healthcare system. Describe the drawbacks of current diagnostic techniques and the potential advantages of automated tools for skin disease detection, such as improved accuracy and effectiveness.

2.5 Challenges

- **Dataset:** The most difficult part of this research is choosing the right dataset.
- **Algorithm Selection:** The object detection model can be trained using a wide variety of algorithms. Therefore, choosing the best algorithm was a difficult task.
- **Preparing data:** A challenge was getting the image data ready for training. As a result, preparing the entire dataset was a difficult task.
- **Training platform:** A high-end processing power would be required for training such a large dataset, which we lacked. To complete the task, we used Google Colab and a Jupyter Notebook with GPU.
- **Implementing:** The model's implementation is another difficult task. Due to the high cost of the testing equipment, we used local computers to measure performance.

Chapter 3

Research methodology

In order to identify the best network based on accuracy and the best transfer learning model for the classification problem, this study looked at five models, as was already indicated. VGG16, VGG19, MobileNetV2, InceptionV3, and MobileNet are a collection of five transfer learning models that have already been trained and tested using test data.

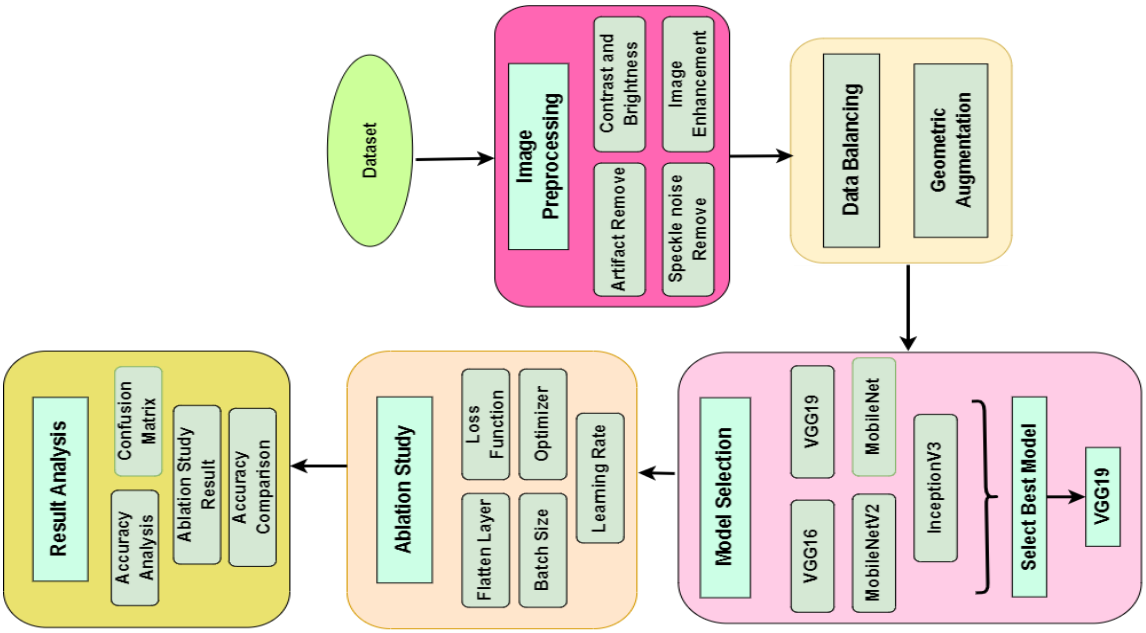

Figure 3: Working flow of the entire classification process

3.1 VGG16

VGG-16 is one of the best models of transfer learning approaches. The DCNN model recognized as VGG16 was first presented by Simonyan and Zisserman [24]. All the hidden layers utilized a nonlinear ReLU activation function, while the top layer used a SoftMax function.

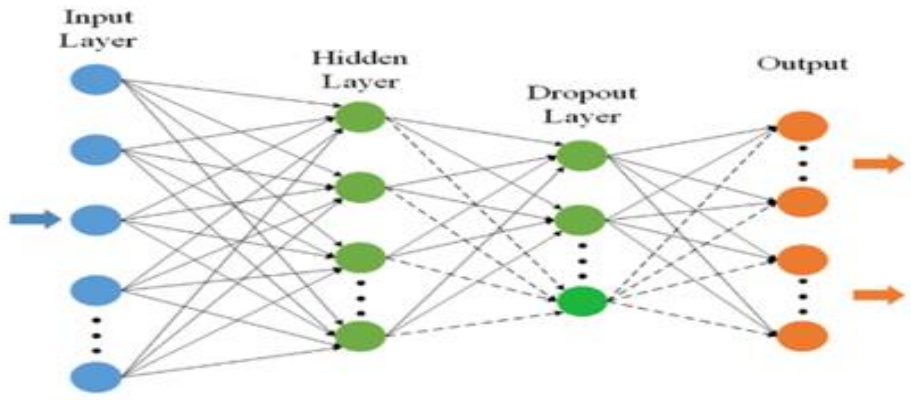

Figure 3.1: VGG-16 Architecture

3.2 VGG19

Numerous millions of image samples were used to train it. The VGG19 model consists of 19 layers. There are two 4096-sized layers in each of the three dense layers, five MaxPool layers, and sixteen convolution layers. All of VGG19's hidden layers, like those of VGG16, use the ReLU activation function, and The top layer use the SoftMax function.

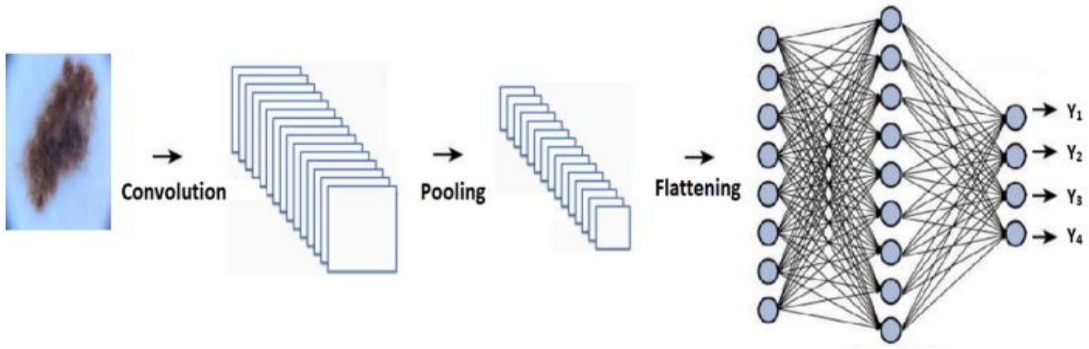

Figure 3.2: VGG-19 Architecture

3.3 MobileNet

This network uses connections that are separable according to depth. The depth wise convolution for MobileNets [25] applies a single filter to each input channel. The pointwise convolution employing a 1 x 1 convolution is then used to combine the outputs of the depth-wise convolution. This is divided into two layers by the depth-wise separable

convolution: a layer for filtering and a layer for combining. This factorization leads to a large reduction in computation and model size.

3.4 MobileNetV2

With the exception of using inverted residual blocks with bottlenecking features and eliminating nonlinearities in narrow layers, MobileNetV2 architecture is very similar to the original MobileNet [26]. Less parameters are present than in the original MobileNet. All input sizes larger than 3232 are supported by MobileNets, and larger image sizes result in better performance. ReLU6 is used in the first layer's 11 convolution, followed by a depth-wise convolution and a final 11 convolutions that lacks an activation function.

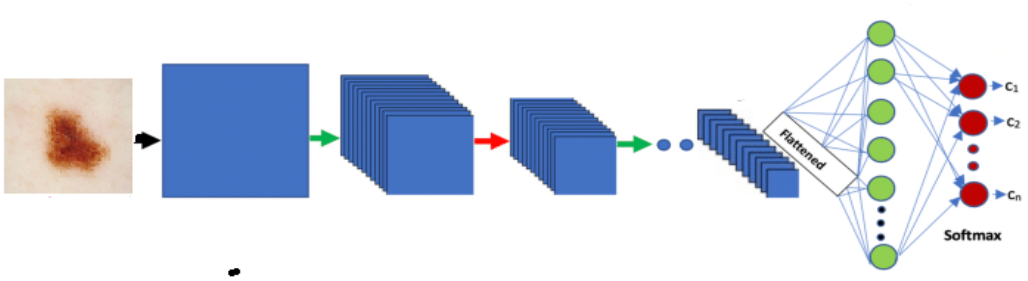

Figure 3.4: MobileNetV2 Architecture

3.5 InceptionV3

This network's main goal is to streamline and streamline this procedure. Regularization, dimension reduction, factorization of convolutions, and parallelization of computations are ways to lower the computational cost. Label information is transmitted down the network using an auxiliary classifier and 77 convolutional layers with label smoothing factorization in InceptionV3. By swapping out larger convolutions for smaller ones, InceptionV3 shortens training time. Within the same network module, convolutions of the sizes 1x1, 3x3, and 5x5 are computed.

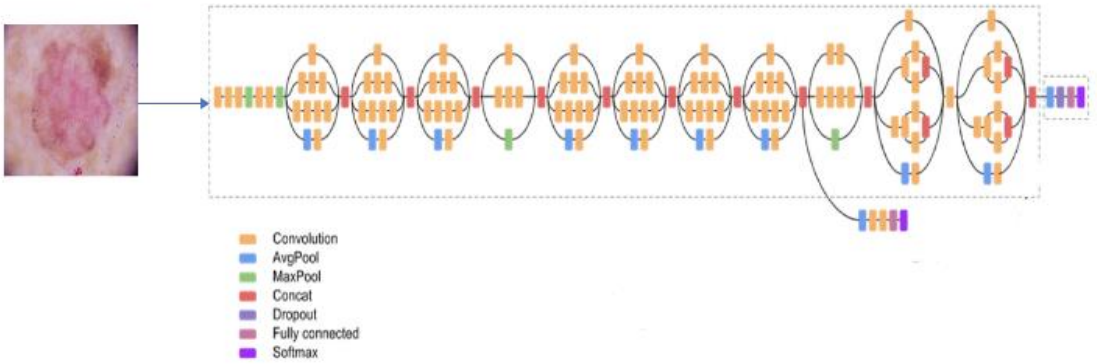

Figure 3.5: InceptionV3 Architecture

3.6 Training Approach

The batch size for training the models is 16, and the highest epoch number is 100[27]. At the time of training the model, callbacks can be used to get a view of the model's internal states and statistics. When you want to automate some tasks that give you control over the training process after each training/epoch, you define and use a callback. The Adam optimizer often outperforms all other optimization methods, requires less tuning, and has a faster computation time. Adam was already employed like an optimizer with a 0.001 learning rate. The standard loss function for multiclass classification is classification cross-entropy [27]. A network's output is standardized via "Softmax" activation to a probability distribution over projected output classes based on Luce's choice axiom. Softmax always has an aggregate of 1, as they normalize all values between 0 and 1.

$$Softmax(y_i) = \frac{\exp(y_i)}{\sum_j \exp(y_i)} \qquad (1)$$

3.7 Ablation Study

The addition of numerous concepts frequently improves the performance of the final model when building a special transfer learning model. To understand the impact of each of these innovations separately in a study, though, is helpful. Researchers frequently evaluate their models with each component disabled in order to gauge the effects of individual components, quantifying the performance loss of the entire model.

3.8 Implementation Requrement

Hardware/Software Requirements

- Minimum Quad Core Processor
- 16 GB RAM
- GTX 1060 GPU
- Operating system
- Minimum 10 GB available Hard Disk

Developing Tools

- Google Colab
- Python Environment
- jupyter notebook
- draw io

Chapter 4

Dataset & preprocessing

4.1 Dataset Description

The dataset was taken from the open-source website Kaggle. A total of 2357 images from the dataset were examined for this study. The dataset includes nine classes: Actinic Keratosis, Basal Cell Carcinoma, Dermatofibroma, Melanoma, Nevus, Pigmented Benign keratosis, Seborrheic Keratosis, Squamous Cell Carcinoma, Vascular lesions. The datasets all images have different size of pixels in grayscale system. The dataset's detailed description is displayed in Table 4.1.

TABLE 4.1: DATASET DESCRIPTION

Name	**Description**
Total Number of Images	2357
Dimension	600 x 450
Data Formats	JPG
Actinic Keratosis	114
Basal Cell Carcinoma	376
Dermatofibroma	95
Melanoma	483
Nevus	357
Pigmented Benign keratosis	462
Seborrheic Keratosis	77
Squamous Cell Carcinoma	181
Vascular lesions	139

Figure 4.1: Skin Cancer Dataset with nine Classes

4.2 Image Preprocessing

The skin disease dataset images contain a lot of noise and artifacts, in order to increase the model's accuracy, this study focuses on image processing. Image processing is frequently thought of as the arbitrary manipulation of an image to meet an aesthetic requirement or to support the desired reality. Image processing is best understood as translating between the human visual system and digital imaging equipment, though. The first step in training a deep learning model is image processing because images include many artifacts. First, we remove artifacts from this image; we use Artifact Removal, Morphological dilation, Remove Spackle Noise, Median Filter, and Clahe Operation.

4.2.1 Morphological Dilation

The skin cancer dataset contains artifacts, and these artifacts are removed using morphological operations [28]. In this study, morphological dilation techniques are used instead of other morphological operations that can be used to remove artifacts. The cv2.getStructuringElement function is used in this study to extract artifact from Figure 4.2.1 and create a rectangular kernel.

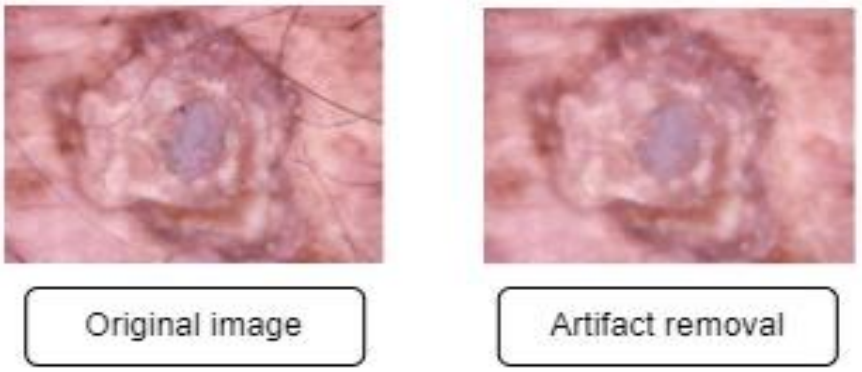

Figure 4.2.1: Output of the morphological dilation

4.2.2 Remove Speckle Noise and Median Filter

The skin diseases dataset contains spackle noise, as was already mentioned. Median filters can eliminate speckle noise. For images with no speckle noise, the median filter is initially applied to this dataset. The median filter is a filtering technique for signal and image noise reduction. In the field of image processing, the median filter is extremely important because it is well known to maintain edges while removing noise. The result of this step is show in the Figure 4.2.2.

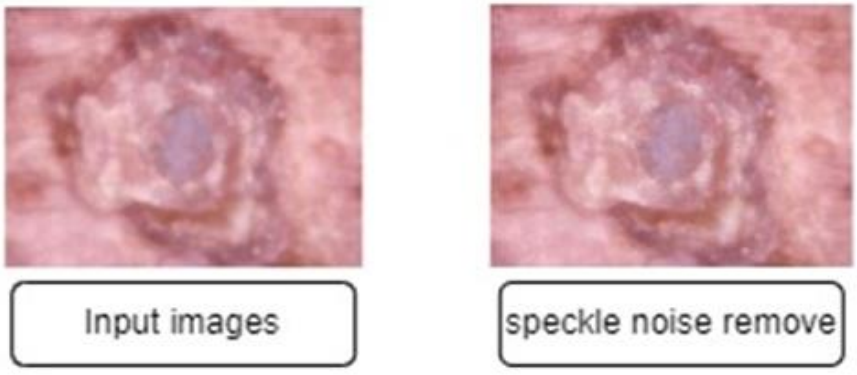

Figure 4.2.2 Output of the Median Filter

4.2.3 Clahe

The original purpose of Clahe was to enhance low-contrast images. In contrast to regular AHE, Clahe restricts contrast. The Clahe implemented a clipping limit to address the issue of noise amplification. The result of this step is show in the Figure 4.2.3.

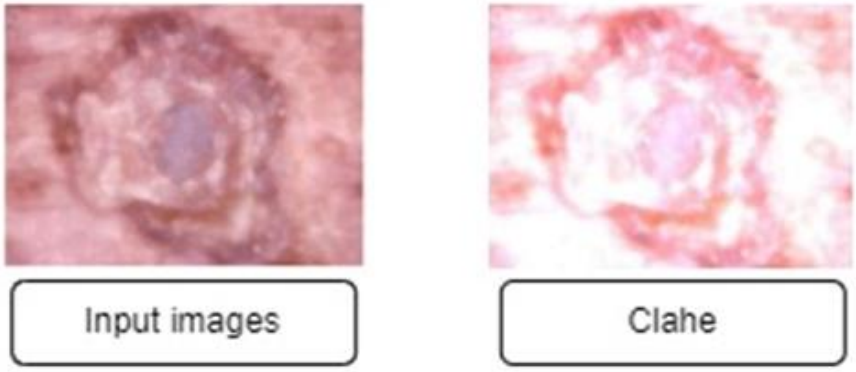

Figure 4.2.3: Output of the Clahe

Let,

Where,

M x M = Image

m x m = tile size of image

$$D = \frac{M \times M}{m \times m} \quad (2)$$

Clip limit $C_L = M_{CL} \times M_{avg}$ is used to construct the statistics for these tiles.

Then,

M_{CL} = Contrast limit.

M_{AVG} = Number of pixels on average

The equation of average pixel is (3):

$$M_{AVG} = \frac{Mx \times My}{Mg} \quad (3)$$

Where,

Mg = Gray level

Mx = Pixel of x dimension

and My = Pixel of y dimension

$$M_{CP} = \frac{M \sum cl}{Mg} \quad (4)$$

Where,

$$M_r = \frac{M_g}{M_r} \quad (5)$$

Where,

M_r is the number of pixels that are still clipped.

Where, P × Q is the image size and L is the highest concentration level and the clahe formula:

$$I_c(p,q) = \mathrm{D}\,(\iota(p,q) = \frac{(L-1)}{PQ}\sum_j^K n_j \quad (6)$$

4.2.4 Alpha-Beta

The images used in this study have their contrast and brightness levels adjusted using alpha and beta correction. To find the desired images, adjust alpha and beta values. The result of this step is show in the Figure 4.2.4.

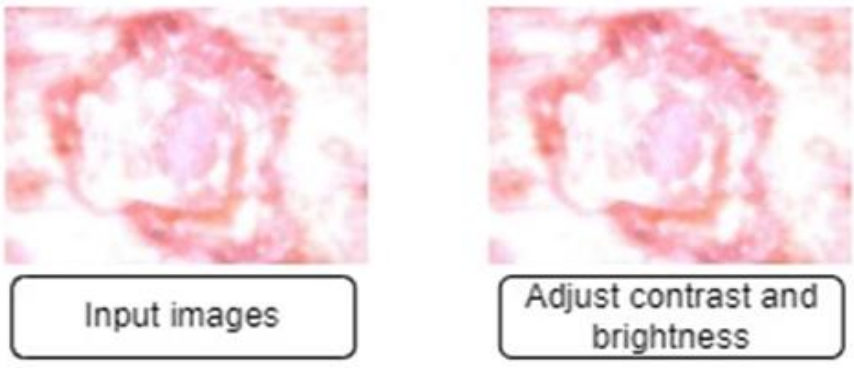

Figure 4.2.4: Output of the alpha and beta

4.2.5 Verification

Required to give that it can viable to lose a large amount of picture quality in using many image preprocessing methodologies, various types of numerical evaluation, such as MSE, RMSE, SSIM, and PSNR, are conducted to ascertain whether the picture quality was already harmed.

4.2.5.1 MSE

Perhaps the most basic and widely used loss function is the Mean Squared Error (MSE), which is frequently covered in introductory machine learning courses. The MSE is calculated by taking the difference between the predictions made by your model and the actual data, squaring it, and averaging it over the entire dataset. The pixels in the two images under comparing have an accumulated squared error, according to MSE. Values near 0 indicate superb image resolution. Noiseless pictures have a value of 0. A value greater than 0.5 denotes a quality decline. Since the MSE gives these errors more weight because of the squaring component of the function, it is excellent for ensuring that our trained model does not contain any outlier predictions with significant errors.

$$MSE = \frac{1}{xy}\sum_{i=0}^{m-1}\sum_{j=0}^{n-1}(O(m,n) - P(m,n))^2 \qquad (7)$$

Where,

O is the ground truth (original image), P is the processed image, x and y denote the pixels of O and P, and m, n denote the rows of the pixels x, y.

4.2.5.2 PSNR

The peak signal-to-noise ratio between two images, measured in decibels, is computed by the PSNR block. This ratio is used to compare the original and compressed images' quality. The quality of the compressed or reconstructed image improves with increasing PSNR. In

order to calculate PSNR, MSE must first be calculated. This is the ratio between the maximum power of a signal and the power of the corrupting noise affecting the quality of an image. The PSNR is then calculated as follows:

$$PSNR = 10\log_{10}\left(\frac{Q^2}{MSE}\right) \quad (8)$$

The input image data type Q has the highest fluctuation. The max is 255 pixels [26].

4.2.5.3 SSIM

A method for estimating the perceived quality of digital television and cinematic images, as well as other types of digital images and videos is the structural similarity index measure (SSIM). SSIM is a tool that determines how similar two images are each other. The SSIM index is a full reference metric, meaning that the initial uncompressed or distortion-free image serves as the baseline for the measurement or prediction of image quality. Preprocessing algorithms reduce image quality, as measured by SSIM. A score of 1 reveals "perfect structural similarity" and a result of 0 indicates no structural similarity [26].

$$SSIM(x,y) = \frac{(2\mu_x\mu_y + c_1)(2\sigma_{xy} + c_2)}{(\mu_x^2 + \mu_x^2 + c_1)(\sigma_x^2 + \sigma_x^2 + c_2)} \quad (9)$$

4.2.5.4 RMSI

RMSE measures up the original and filtered images to determine an image's quality. A RMSE value that is close to 0 denotes an accurate image with few errors.

$$RMSE = \sqrt{\sum_{J=1}^{N}(d_{fi} - \frac{d_d)^2}{N}} \quad (10)$$

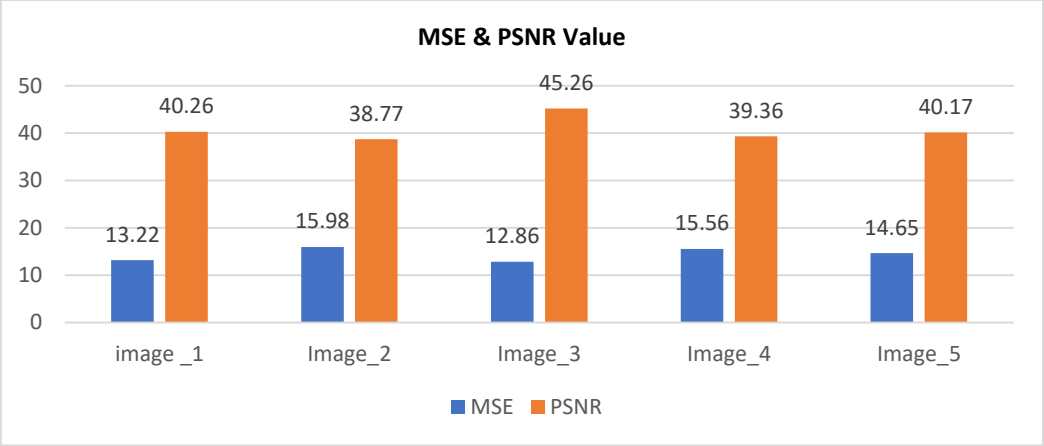

Figure 4.2.5.1: MSE & PSNR Value for Five Images

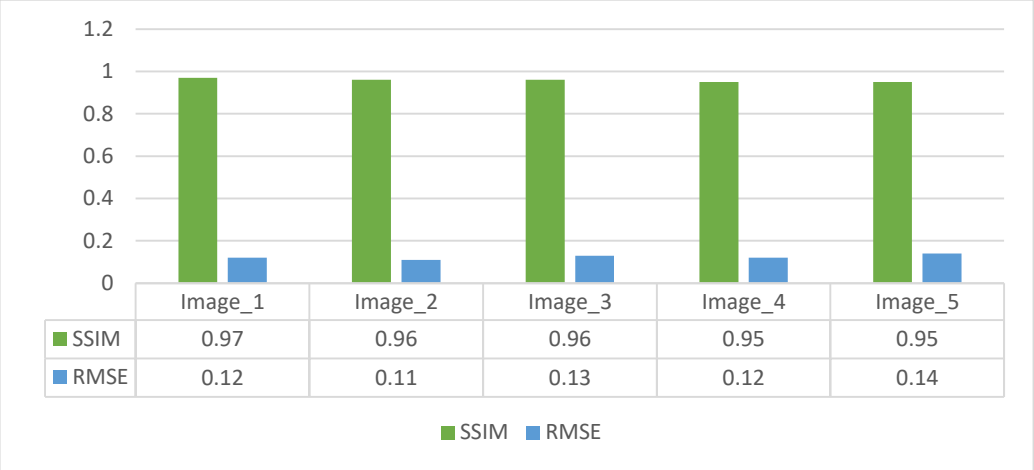

Figure 4.2.5.2: SSIM & RMSE Value for Five Images

4.3 Data Split

The dataset must be split before training. Three different splitting ratios are frequently employed in studies to evaluate the model's accuracy, depending on how much data there is for training and testing (90:10, 80:20, and 70:30). To make the final prediction, 20% of the dataset was used as the test dataset in a recent study [28]. The ratio of the three sets of images for the training, validation, and test sets, respectively, was 70:10:20.

Chapter 5

Result & discussion

5.1 Result of Transfer Learning Model

The test accuracy, Validation accuracy, and training accuracy are displayed in Fig. 5.1.1. Fig. 5.1.2 displays the validation, train, and test loss for the five transfer learning models. As seen in Fig. 5.1.1, the VGG-19 model has the highest accuracy.

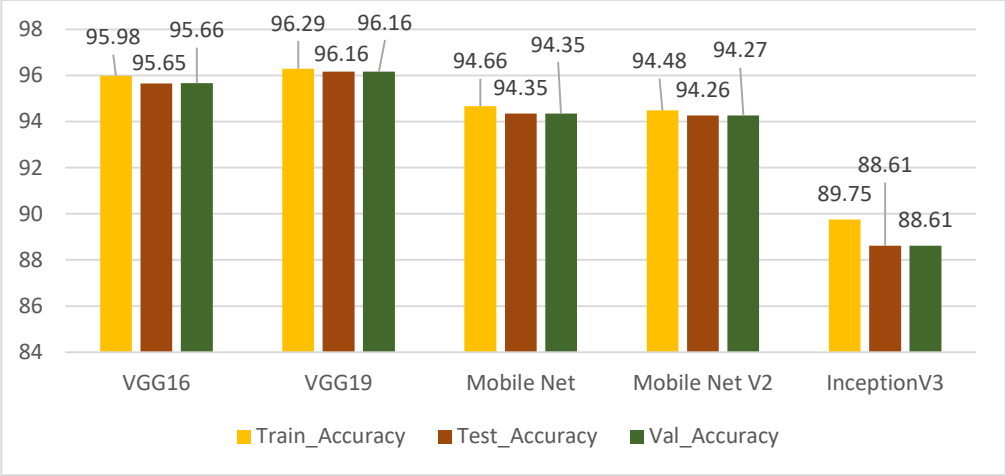

Figure 5.1.1: Train Accuracy, Test Accuracy and Val Accuracy for five Transfer Learning Model

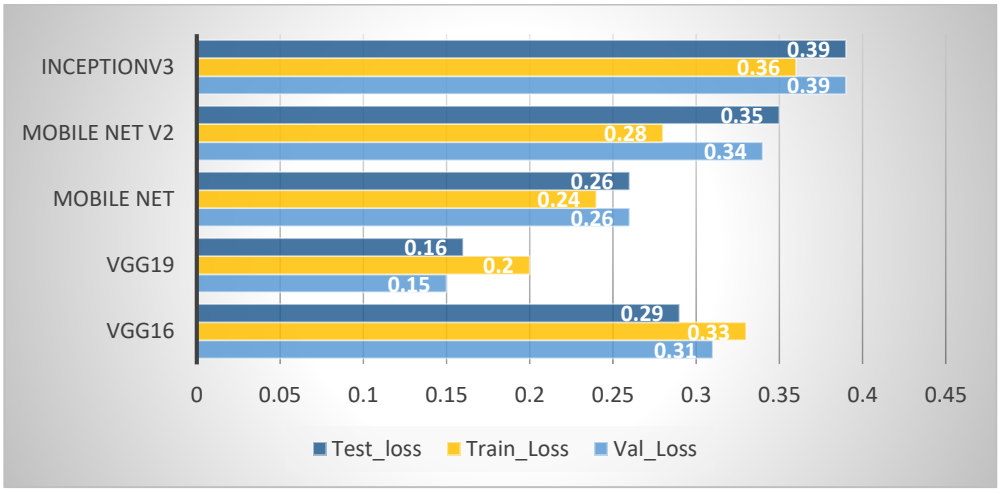

Figure 5.1.2: Test, Val and Train Loss for five Transfer Learning Model

5.2 Result of Ablation Study

By altering a few design elements, classification accuracy can be increased and reliability increased. The optimized VGG19 architecture is used to modify various elements across five studies that make up the ablation study.

5.2.1 Changing Flatten Layer

As seen in Figure 5.2.1, by using flatten layer provides the greatest accuracy. The Global Maximum Pooling and Global Average Pooling both provide poor accuracy. When the layer is flattened, its accuracy is 96.29%; when it is global maximum pooling, it is 92.65%; and when it is global average pooling, it is 90.52%.

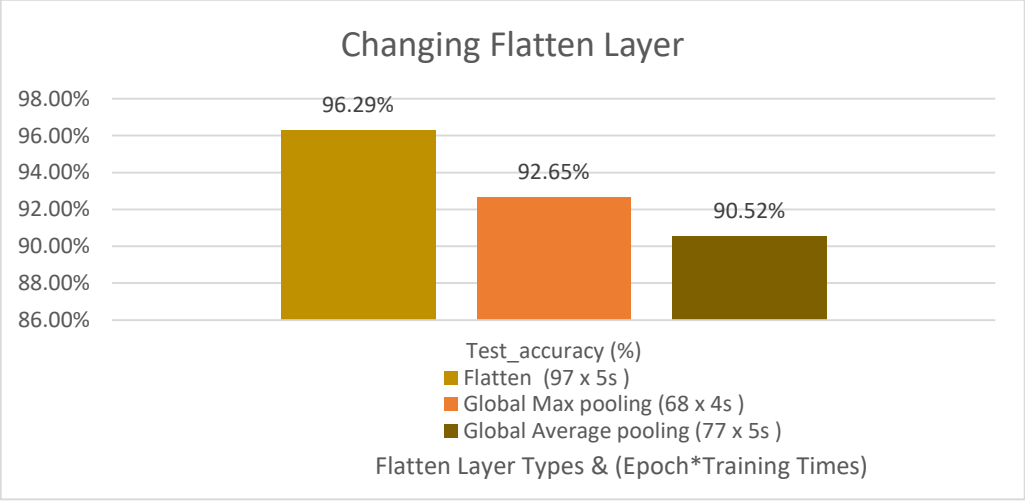

Figure 5.2.1: Changing Flatten Layer

5.2.2 Changing The Batch Size

When batch size 32 was used, we found the highest accuracy, as shown in Figure 5.2.2. Furthermore, batch size 16 and batch size 64 offer poor accuracy. The accuracy is 97.16% when the batch size is 32, 94.55% when the batch size is 64, and 96.29% when the batch size is 16.

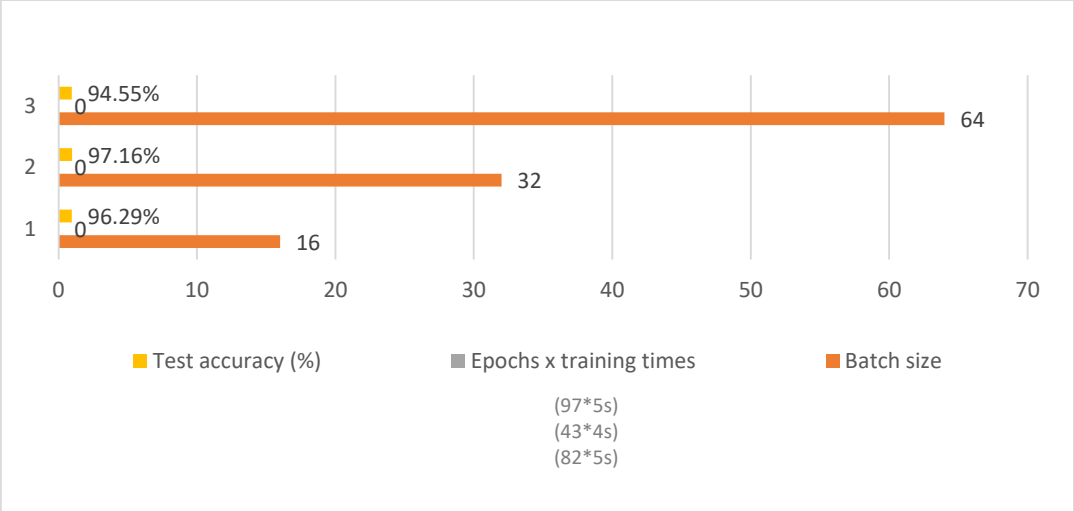

Figure 5.2.2: Change the Batch Size

5.2.3 Changing the Loss Function

When we alter the loss functions, categorical cross-entropy produces the best accuracy 97.16%.

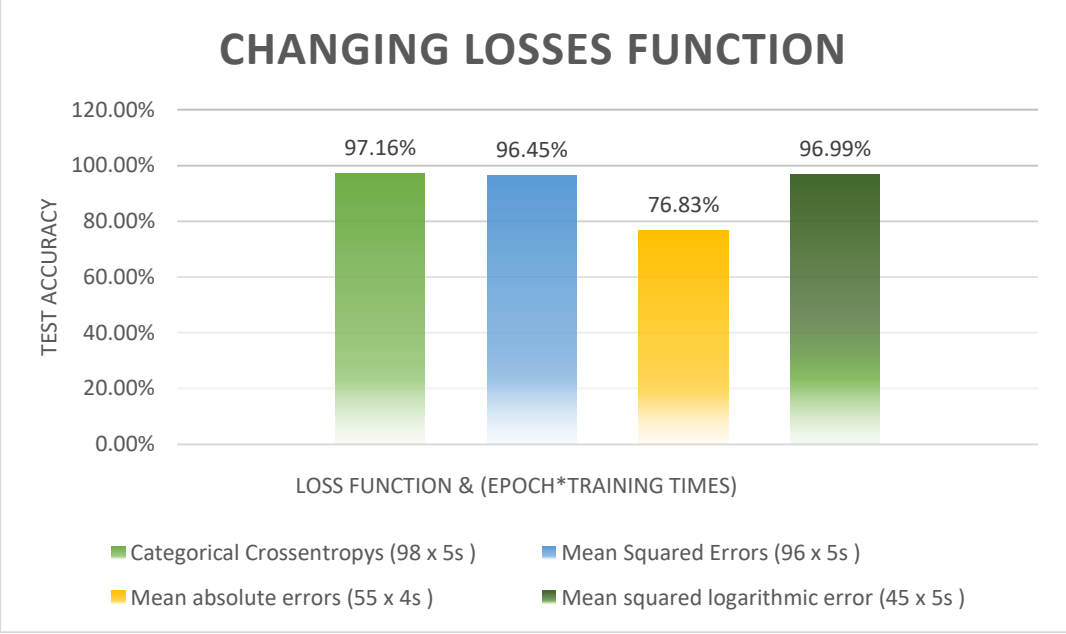

Figure 5.2.3: Changing Losses Function

5.2.4 Changing Optimizers

In comparison to the optimizers Nadam, SGD, and Adamax shown in figure 5.2.4, Adam optimizer offers the highest accuracy.

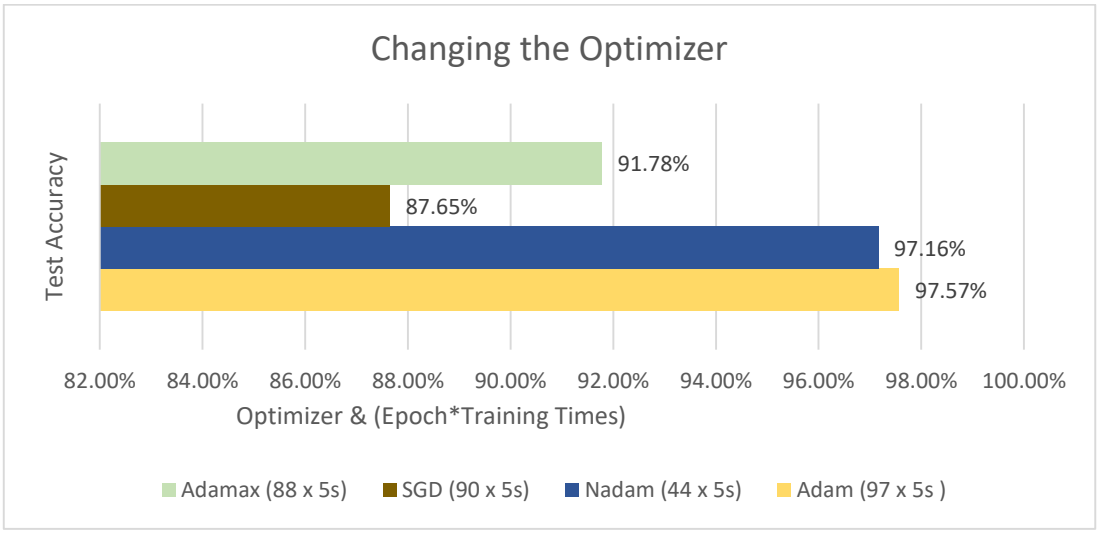

Figure 5.2.4: Changing the Optimizer

5.2.5 Changing Learning Rate

When using 0.001 as opposed to 0.001, 0.0001, and 0.01, the accuracy is the highest.

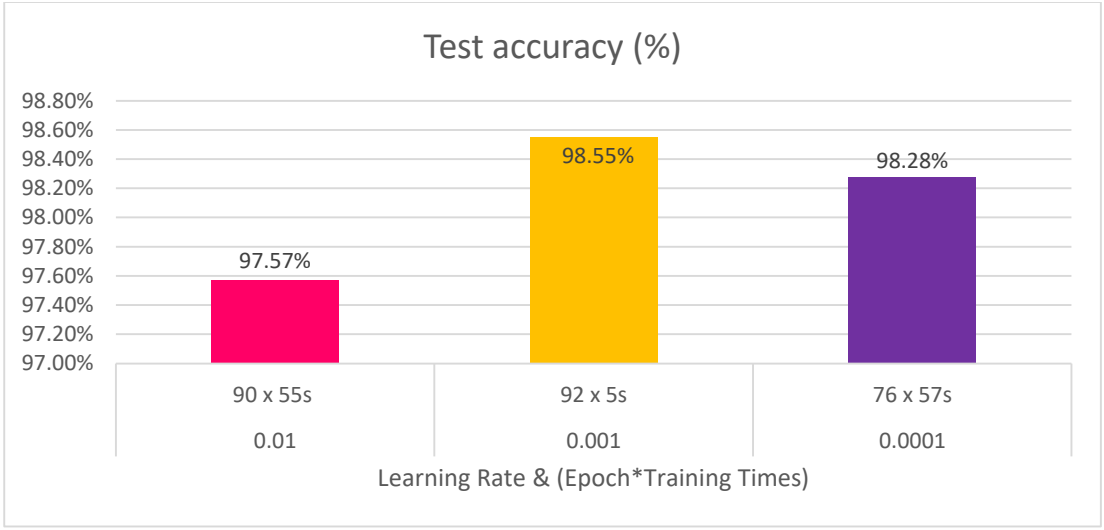

Figure 5.2.5: Changing Learning Rate

5.2.6 Performance Analysis of Best Model

Table 5.2.6 provides an overview of the final configuration of VGG19.

TABLE 5.2.6: CONFIGURATION OF OUR MODEL

Configuration	Value
Image sizes	224 x 224
Epochs	90
Optimization Functions	Adam
Learning rates	0.001
Batch sizes	32
Activation functions	Softmax
Dropouts	0.5
Momentums	0.9
Accuracy	98.55

5.2.7 Performance analysis and statistical analysis

The RMSE, MAE, MCC, KC, FDR, FNR, FPR, Accuracy, Precession, Recall, Specificity, and F1 Score of the greatest hyper-tuned VGG19 method are shown in Figures 5.2.7.1 and 5.2.7.2.

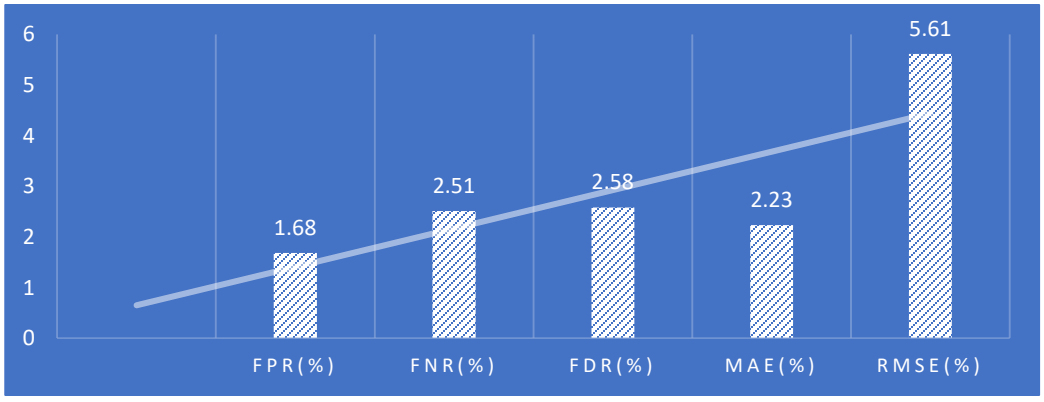

Figure 5.2.7.1: FPR, FNR, FDR, MAE, RMSE (%) Value of VGG19 model

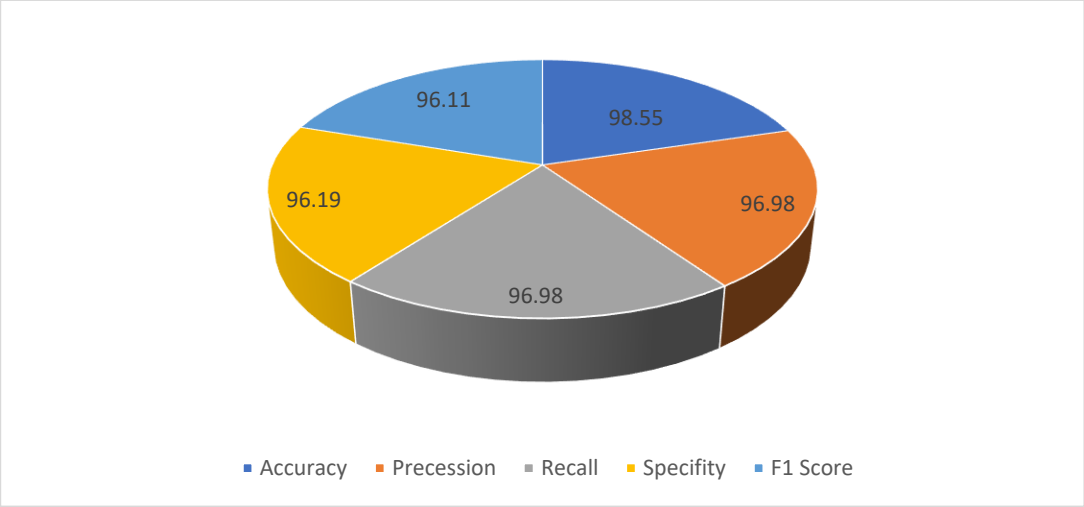

Figure 5.2.7.2: Accuracy, F1 score, Specifity, Recall, Precession Value of VGG19 model

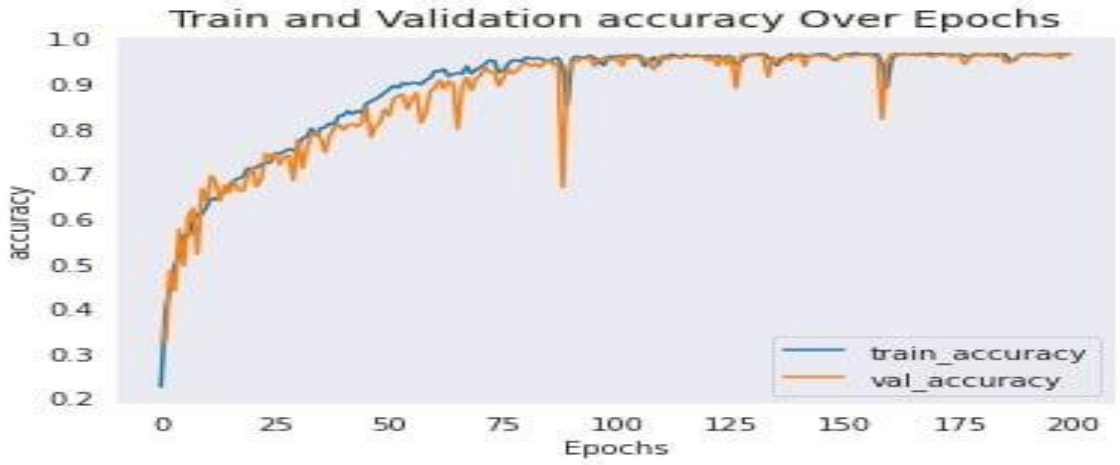

Figure 5.2.7.3: Accuracy curves

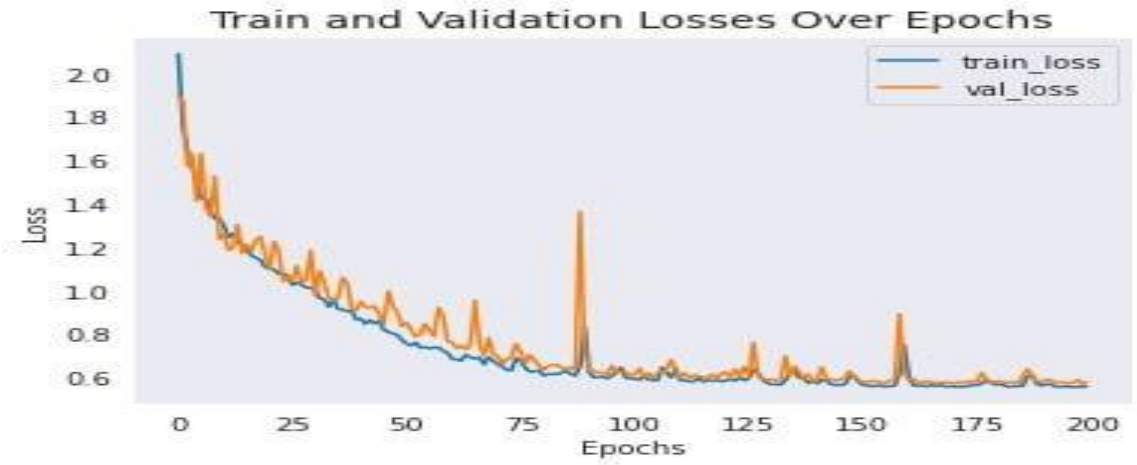

Figure 5.2.7.4: Loss curves

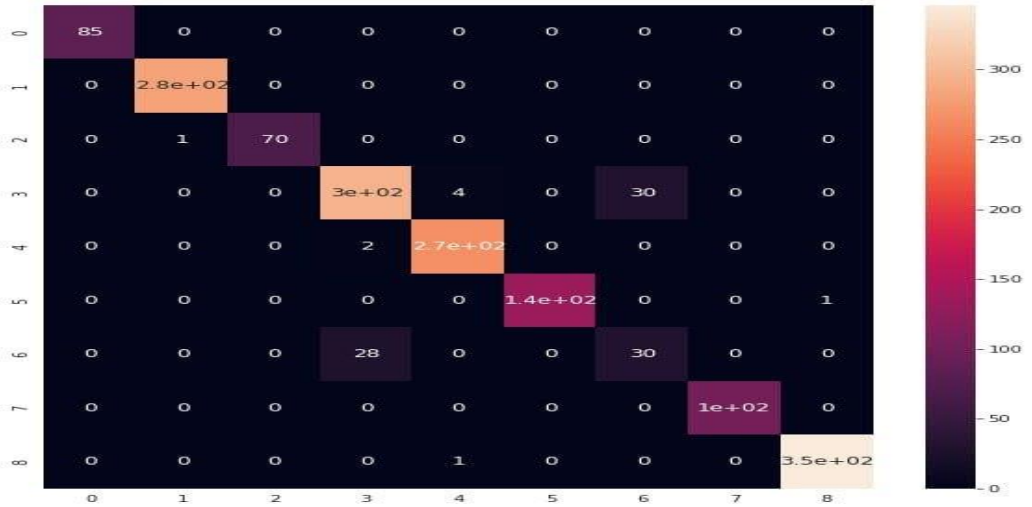

Figure 5.2.7.5: Confusion Matrix

Chapter 6

Impact on Society, Environment and Sustainability

6.1 Impact on Society

Using automated diagnostic tools, like the tuned VGG-19 model, can increase the precision with which skin diseases are found. This can ensure that patients get the right care when they need it, improving outcomes and lowering the chance of complications. The use of automated diagnostic tools can expand access to care for patients who may not have previously had access to specialized medical knowledge in remote or resource-constrained areas.

6.2 Impact on Environment

Our research based project does not use anything that will harm the environment. There are some beneficial social effects of our project. Society and the environment are interdependent, even in small doses. Therefore, the environment will gain significantly if society can improve.

6.3 Ethical Aspects

Our project has a positive effect on moral considerations, such as early detection and prevention of skin cancer. It will be morally correct if it can achieve the precise goal for which this project was created.

6.4 Sustainability Plan

It is crucial to keep gathering new data and updating the training dataset in order to make sure the model is accurate and current. This could involve adding new skin disease images to the training dataset on a regular basis, annotating them, and doing so. The model's performance should be regularly evaluated, and any problems or potential improvements

should be found. This may entail studying the model's performance metrics and getting user input. In order to maintain the model's proper operation, it is crucial to provide technical support. This can involve routine software maintenance and updates, as well as troubleshooting and resolving any arising technical issues. It will be necessary to retrain the model on the updated dataset in order to keep it current with new data. The amount of time between retraining sessions will depend on how quickly the data change and what performance level is desired.

Chapter 7

Conclusion, Limitation & Future Work and Summary of the study

7.1 Conclusion

This paper proposes a convolutional neural network-based method for the transfer learning classification of skin diseases. A method has been developed that may assist both people and medical professionals in detecting skin cancer classes, regardless of whether the cancer is benign or malignant. A conclusion that can be drawn from the experimental and assessment phase is that the model may be regarded as a standard for diagnosing skin diseases by providing assistance to medical experts. Any physician may recognize the proper findings by capturing a few random photos, but the old technique takes too much time to determine whether or not a case has been correctly identified

7.2 Limitation & Future Work

Transfer learning models performed significantly better for multiclass classification in this study than traditional classifiers. Despite the research's serious flaw—the loss of a sizable amount of accurate medical data—the dataset for the proposed model is not large enough. In the not-too-distant future, larger volumes of unanalyzed medical images combined with real-time medical data may be used to assess the performance of the proposed model. However, the majority of tests indicate that the model presented in this study accurately categorizes the four distinct types of skin diseases. It may have a few minor issues, but it is not impossible. It is not possible to ensure that the suggested fine-tuned VGG19 model is correct and enhanced across all aspects of diagnosis, despite a few minor flaws. It is possible to accomplish this. The clinical use of deep learning for the diagnosis of more disorders can be investigated in future studies. For relatively uncommon diseases, transfer learning may be helpful. Additionally, models might develop to require fewer preprocessing steps. Along with these, a deeper comprehension of the reconstruction kernel or image thickness might enhance the performance of deep learning models.

7.3 Summary of the Study

Numerous experiments demonstrate how capable our model is. In picture frames, it is able to find skin cancer. We are working to put a transfer learning method from images into practice. We've done data collection, data filtering, and data resizing first. Then, using image processing software, divide the data into training, validation, and test sets.

The dataset was then run through a transfer learning model, and the accuracy of each algorithm was then provided. The accuracy was then calculated in order to improve the VGG19 model's performance. Then we, Ablation study on the best performance model.

7.4 Implication for further studies

Our system was designed with a variety of possible future applications. A complete system can be created if the dataset can be enhanced with more pertinent classes and images. The VGG19 algorithm is already faster and has produced excellent results; if we can further reduce its complexity, it will perform even better.

References

[1] Sung H, Ferlay J, Siegel RL, Laversanne M, Soerjomataram I, Jemal A, et al. Global cancer statistics 2020: GLOBOCAN estimates of incidence and mortalityworldwide for 36 cancers in 185 countries. CA Cancer J Clin (2020) 71:209–49.doi: 10.3322/caac.21660

[2] Bray F, Ferlay J, Soerjomataram I, Siegel RL, Torre LA, Jemal A. Globalcancer statistics 2018: GLOBOCAN estimates of incidence and mortalityworldwide for 36 cancers in 185 countries. CA Cancer J Clin (2018) 68:394–424.doi: 10.3322/caac.21492

[3] World Cancer Research Func. "Skin cancer statistics". UK: AmericanInstitute for Cancer Research. (2020). Available at: https://www.wcrf.org/dietandcancer/skin-cancer-statistics/.

[4] Cancer Research UK. "Cancer incidence statistics". Available at: https://www.cancerresearchuk.org/health-professional/cancer-statistics/incidence.

[5] The global cancer observatory: Bangladesh march (2021). Available at:https://gco.iarc.fr/today/data/factsheets/populations/50-bangladesh-fact-sheets.pdf.

[6] Bangladesh: Skin cancers by world health organization (2018). Available at:https://www.worldlifeexpectancy.com/bangladesh-skin-cancers.

[7] Beeravolu AR, Azam S, Jonkman M, Shanmugam B, Kannoorpatti K, AnwarA. "Preprocessing of breast can-cer images to create datasets for deep-CNN," Vol. vol.9. United Sates: IEEE (2021) p. 33438–63. doi: 10.1109/ACCESS.2021.30587738.

[8] Ghosh P, Azam S, Hasib KM, Karim A, Jonkman M, Anwar A. "Aperformance based study on deep learning algorithms in the effective predictionof breast cancer,"IJCNN. United Sates: International Joint Conference on NeuralNet-works (2021).

[9] M. Berseth, "ISIC 2017 - skin lesion analysis towards melanoma detection," 2017.

[10] X. Dai, I. Spasic, B. Meyer, S. Chapman, and F. Andres, "Machine learning on mobile: An on-device inference app for skin cancer detection," in Fourth International Conference on Fog and Mobile Edge Computing (FMEC), 2019, pp. 301–305.

[11] P. Tschandl, "The HAM10000 dataset, a large collection of multisource dermatoscopic images of common pigmented skin lesions," 2018. [Online]. Available: https://doi.org/10.7910/DVN/DBW86T

[12] A. G. Pacheco, G. R. Lima, A. S. Salomao, B. Krohling, I. P. Biral, ˜ G. G. de Angelo, F. C. Alves Jr, J. G. Esgario, A. C. Simora, P. B. Castro et al., "Pad-ufes-20: A skin lesion dataset composed of patient data and clinical images collected from smartphones," Data in Brief, vol. 32, p. 106221, 2020.

[13] Esteva A, Kuprel B, Novoa R, Ko J, Swetter SM, Blau HM, et al. Correction:Corrigendum: Dermatologist-level classification of skin cancer with deep neuralnetworks. Nature (2017) 546:686. doi: 10.1038/nature22985

[14] Jinnai S, Yamazaki N, Hirano Y, Sugawara Y, Ohe Y, Hamamoto R. Thedevelopment of a skin cancer classifi-cation system for pigmented skinlesions using deep learning. Biomolecules (2020) 10:1–13. doi: 10.3390/biom10081123

[15] G. Argenziano and H. P. Soyer, “Dermoscopy of pigmented skin lesions–a valuable tool for early diagnosis of melanoma,” The Lancet Oncology, vol. 2, no. 7, pp. 443–449, 2001.

[16] H. Kittler, H. Pehamberger, K. Wolff, and M. Binder, “Diagnostic accuracy of dermoscopy,” The lancet oncology, vol. 3, no. 3, pp. 159–165, 2002

[17] “International Skin Imaging Collaboration: Melanoma Project Website,” https://isic-archive. com/.

[18] “IEEE International Symposium on Biomedical Imaging,” http://biomedicalimaging.org/.

[19] Ashraf R, Afzal S, Rehman AU, Gul S, Baber J, Bakhty M, et al. “Region-of-Interest based transfer learning assisted framework for skin cancer detection,” Vol. 8. United States: IEEE (2020) p. 147858–71. doi: 10.1109/ACCESS.2020.3014701

[20] Goyal M, Yap MH. “Region of interest detection in dermoscopic images fornatural data-augmentation,”. United States: arXiv (2018) p. 1–8.

[21] Ali AR, Li J, Kanwal S, Yang G, Hussain A, Jane O’Shea S. A novel fuzzymultilayer perceptron (F-MLP) for the detection of irregularity in skin lesionborder using dermoscopic images. Front Med (2020) 7:297. doi: 10.3389/fmed.2020.00297

[22] Fujisawa Y, Inoue S, Nakamura Y. The possibility of deep learning-based,computer-aided skin tumor classi-fiers. Front Med (2019) 6:191. doi: 10.3389/fmed.2019.00191

[23] Alizadeh SM, Mahloojifar A. Automatic skin cancer detection indermoscopy images by combining convolutional neural networks and texturefeatures. Int J Imaging Syst Technol (2021) 31:695–707. doi: 10.1002/ima.22490Ghosh et al. 10.3389/fonc.2022.931141Frontiers in Oncology frontiersin.org20-6

[24] Wang, P.; Wang, J.; Li, Y.; Li, P.; Li, L.; Jiang, M. Automatic classification of breast cancer histopathological images based on deep feature fusion and enhanced routing. Biomed. Signal. Process. Control 2021, 65, 102341.

[25] Howard, A.G.; Zhu, M.; Chen, B.; Kalenichenko, D.; Wang, W.; Weyand, T.; Andreetto, M.; Adam, H. Mobilenets: Efficient convolutional neural networks for mobile vision applications. arXiv 2017, arXiv:1704.04861.

[26] Sandler M, Howard A, Zhu M, Zhmoginov A, Chen L.-C (2018) Mobilenetv2: Inverted residuals and linear bottlenecks. In: Proceedings of the IEEE conference on computer vision and pattern recognition, pp 4510–4520

[27] Shallu; Mehra, R. Breast cancer histology images classification: Training from scratch or transfer learning? ICT Express 2018, 4, 247–254.

[28] Abbas, A.H.; Kareem, A.A.; Kamil, M.Y. Breast Cancer Image Segmentation Using Morphological Operations. Int. J. Electron. Commun. Eng. Technol. 2015, 6, 8–14.

[27] Van Droogenbroeck, M.; Buckley, M.J. Morphological Erosions and Openings: Fast Algorithms Based on Anchors. J. Math. Imaging Vis. 2005, 22, 121–142.

[28] Beeravolu, A.R.; Azam, S.; Jonkman, M.; Shanmugam, B.; Kannoorpatti, K.; Anwar, A. Preprocessing of Breast Cancer Images to Create Datasets for Deep-CNN. IEEE Access 2021, 9, 33438–33463.

[29] Lee T, Ng V, Gallagher R, Coldman A, McLean D. Dullrazor: A softwareapproach to hair removal from images. Comput BiolMed (1997) 27(6):533–43.doi: 10.1016/s0010-4825(97)00020

Habib

ORIGINALITY REPORT

18%	13%	11%	8%
SIMILARITY INDEX	INTERNET SOURCES	PUBLICATIONS	STUDENT PAPERS

PRIMARY SOURCES

1	Submitted to Daffodil International University Student Paper	2%
2	dspace.daffodilvarsity.edu.bd:8080 Internet Source	2%
3	www.frontiersin.org Internet Source	2%
4	Md Harun or Rashid, Salma Akter, Amatul Bhusra Akhi. "BrainNet-7: A CNN Model for Diagnosing Brain Tumors from MRI Images based on an Ablation Study", International Journal of Advanced Computer Science and Applications, 2022 Publication	1%
5	Submitted to De Montfort University Student Paper	1%
6	www.mdpi.com Internet Source	1%
7	www.ijraset.com Internet Source	1%